Article

Geometrical Isomerism in Guanabenz Free Base: Synthesis, Characterization, Crystal Structure and Theoretical Studies

Deepika Kathuria, Sumit S. Chourasiya, Aabid Abdullah Wani, Manjeet Singh, Subash C. Sahoo, and Prasad V. Bharatam

Cryst. Growth Des., **Just Accepted Manuscript** • DOI: 10.1021/acs.cgd.9b00026 • Publication Date (Web): 02 May 2019

Geometrical Isomerism in Guanabenz Free Base: Synthesis, Characterization, Crystal Structure and Theoretical Studies

Deepika Kathuria,[†] Sumit S. Chourasiya,[†] Aabid Abdullah Wani,[†] Manjeet Singh, [§]

Subash C. Sahoo[*§] and Prasad V. Bharatam*[*†]

[†]Department of Medicinal Chemistry, National Institute of Pharmaceutical Education and Research (NIPER), Sector 67, S. A. S. Nagar – 160062, Punjab, India

[§]Department of Chemistry, Panjab University Chandigarh, Sector-14, Chandigarh, 160014, India

KEYWORDS: Guanabenz, Isomerism, Crystal Structure, Polymorphism, DFT

ABSTRACT: Guanabenz is a drug used for the treatment of hypertension, it exhibits isomerism and tautomerism. In this article, X-Ray diffraction studies (single crystal and powder), as well as thermochemical analysis on the guanabenz have been reported. The results indicated that *E*/*Z* isomerism in guanabenz is responsible for the identification of two solid forms, Form I (*E*-isomer) and Form II (*Z*-isomer). These two forms may be treated as geometrical polymorphs. Form I of guanabenz was already known. Identification of Form II and its X-Ray structure are reported first time in this article. Quantum chemical analysis and 2D fingerprint plots as Hirshfeld surfaces of these two forms highlight the differences in intermolecular hydrogen bonding, energy differences and π- stacking interactions. The quantum chemical studies indicate that Form-I (*E* isomer) is more stable than Form-II (*Z* isomer) by 2.13 kcal/mol. The presence of Form II in the crystal structure has been rationalized by quantum chemical calculations on the basis of dimerization energies

which suggest that the dimer of *Z* isomer is more stable than the dimer of the *E* isomer by ~7 kcal/mol.

Introduction

In a search for new and better antihypertension drugs during 1960's, a series of benzylidene aminoguanidines were synthesized by Wyeth Laboratories, Inc., Philadelphia. One of the compounds of this series, Wy-8678 (*E*-2,6-dichlorobenzylidene aminoguanidine acetate, **1**, Figure 1) was identified as a new potent hypotensive agent in 1969.[1] The common name given to this compound was guanabenz due to the presence of guanidine and benzylidene moieties. Its antihypertensive action is attributed towards its high affinity to α2-adrenergic receptor.[2] Subsequently, the clinical trials were carried out and guanabenz stands out the most potent compound of the series.[3,4] Guanabenz acetate (**1**) is now in use for the treatment of hypertension and is sold under the brand names Wytensin, Rexitene, Hipten, etc.[4] Apart from the anti-hypertensive activity of guanabenz, it has also been reported for the treatment of various diseases such as cutaneous cystic fibriosis,[5,6] amyloidosis,[7] prion-based diseases,[8-10] inflammation etc.[11,12]

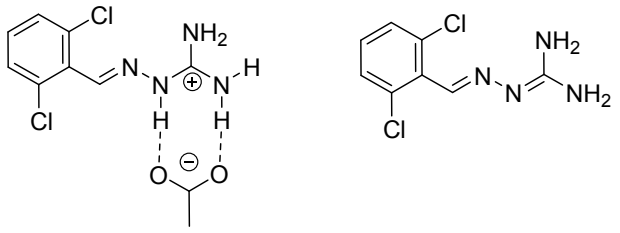

1
Wy-8678
(Guanabenz acetate)

2
(Guanabenz free base)

Figure 1. The structure of guanabenz acetate (**1**) and guanabenz free base (**2**).

Due to the presence of highly basic guanidine moiety in guanabenz, it is marketed as an acetate salt for oral administration (Figure 1). The presence of imine (–CH=N) and guanidine structural moieties in guanabenz attracted researchers to study its structural properties. The (*E*/*Z*) isomerization study on guanabenz acetate and its derivatives was carried out in 1976 by Tsuijkawa

et al.[13] The authors suggested that the *E*-isomer of guanabenz acetate (colourless needle) can easily isomerize to *Z*-isomer (pale yellow powder) by irradiation of U.V. rays on aqueous and methanol solution. The structural differences between *E*/*Z* isomers were established by Nuclear Overhauser Effect (NOE) experiments.[13] These observations were also supported by Holzer and Gyorgydeak in 1992 in their study on the structure of various guanylhydrazones obtained from aromatic aldehydes.[14] Recently, in 2008, a crystal structure of acetate salt of guanabenz (**1**) has been reported by Tanaka and Hirayama.[15] The single crystal X-ray structure of guanabenz acetate indicates that guanabenz (base) and acetic acid are connected by two hydrogen bonds (Figure 1) and the entire salt lies substantially within a single plane.[15]

Although, guanabenz is marketed in its monoprotonated form but its free base (**2**) cannot be ignored, since the available literature on the biological activity of guanabenz and other guanylhydrazone hydrochloride suggested the existence of considerable portion (~16 %) of free base at physiological temperature (~37 °C) and pH (7.4).[16,17] A few studies were reported on the structural aspects of the free base of guanabenz which includes (i) conformational analysis of both monoprotonated as well as free base of guanabenz,[16] the single crystal X-Ray diffraction analysis of *E*-isomer of Guanabenz (its details are not available in CCDC)[16] (ii) the experimental and quantum chemical studies on guanabenz to understand prototropic tautomerism.[18,19] Recently, we have investigated the tautomerism,[18,19] isomerism[20] and medicinal applications[21] of azines and concluded that guanylhydrazones exist preferentially in their azine tautomeric state with *E*-geometry across -C=N, which were evidenced by analyzing the crystal structures.

The quantum chemical studies on guanabenz also suggested that, it prefers to exist in the azine tautomeric state (ΔG = 5.96 kcal/mol) in comparison to its hydrazone tautomeric state. It was found that the azine tautomer of guanabenz carries very interesting properties as it possess

two imine bonds linked by N-N single bond. The conjugation[22] vs. conjugation stopper property[23] vs. conjugation switch property[24] across azines was explored using structural studies (X-rays and quantum chemical). In addition, polymorphism and conformation isomerism in azines was also reported earlier by Glaser and co-workers.[25] Taking these facts together it can be considered that guanabenz can also show *E*/*Z* isomerisation or/and polymorphism (Figure 2). This proposition prompted us to carry out the solid state and computational studies on guanabenz free base.

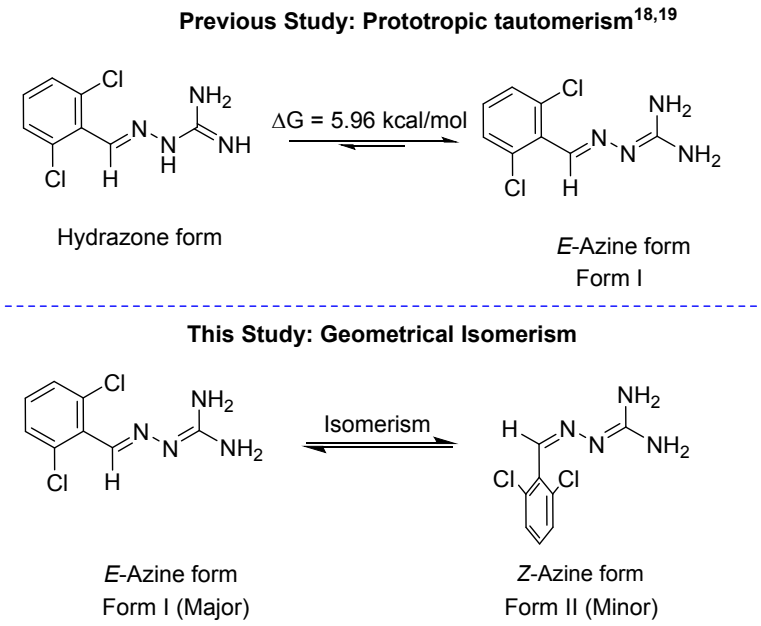

Figure 2. Tautomerism and Geometrical Isomerism in guanabenz free base.

Experimental Section

Materials and Methods

The reagents and chemicals required for the study were procured from Sigma Aldrich and were used as such without further purification unless otherwise mentioned. The progress of the reaction was monitored by Thin Layer Chromatography (TLC) performed on silica gel aluminium plates and visualization was done by UV light. ^{1}H NMR (400 MHz) and ^{13}C NMR (101 MHz) spectra were recorded on a Bruker Advance spectrometer with TMS as an internal standard. The

^{1}H NMR and ^{13}C NMR spectra were recorded for DMSO-*d6* at 2.50 ppm and 39.51 ppm respectively. Chemical shift (δ) values are reported in part per million (ppm). Coupling constants (J) were reported in Hertz (Hz). The abbreviations used to characterize the signals are as follows: s = singlet, d =doublet, t = triplet, br s = broad singlet. High resolution mass spectra were taken using ESI-TOF method. Mass spectra were recorded using ESI mode. The IR spectra were recorded on Thermo Scientific (NICOLET IS50) FT-IR spectrophotometer in the range 4000-400 cm^{-1}.

X-ray Crystallography

Crystals were mounted on Hampton cryoloops. All geometric and intensity data for the crystals were collected using a Super-Nova (Mo) X-ray diffractometer equipped with a micro-focus sealed X-ray tube Mo-Kα (λ = 0.71073 Å) X-ray source, and HyPix3000 (CCD plate) detector of with increasing ω (width of 0.3_ per frame) at a scan speed of either 5 or 10 s/frame. The CrysAlisPro software was used for data acquisition, and data extraction. Using Olex2,[26] the structure was solved with the SIR2004[27] structure solution program using direct methods and refined with the ShelXL[28] refinement package using Least Squares minimization. All non-hydrogen atoms were refined with anisotropic thermal parameters. Details of crystallographic data and structural refinement parameters are summarized in Table S1. Bond angle and bond length geometric parameters are listed in Table S2.

Powder X-ray Diffraction

Powder X-ray Diffraction (PXRD) patterns were recorded on a Phillips PAN analytical diffractometer for Cu Kα radiation (λ = 1.5406 Å), with a scan speed of 2° min^{-1} and a step size of 0.02° in 2θ.

Thermal Analysis

Thermal analysis methods were used in this study which includes thermogravimetric analysis (TGA) and differential scanning calorimetry (DSC). Thermal gravimetric analysis was carried out using Mettler Toledo instrument with an SDTA sensor by loading over an alumina pan and heating from 30 ˚C to 1000 ˚C at a heating rate of 10 ˚C min^{-1} under N_2 atmosphere. DSC was performed using a Mettler-Toledo DSC-821 differential scanning calorimeter). Indium was used for calibration. Accurately weighed samples (5-8 mg) were placed in hermetically sealed aluminum pans and scanned at 10 °C/min under a nitrogen purge. The powders of the Form I and Form II were heated at 10 °C/min. 2D fingerprint plots as Hirshfeld surfaces were calculated using crystalexplor software.[29]

Computational Methods

The quantum chemical calculations were carried out using the Gaussian09 package.[30] Geometry optimizations were carried out by DFT[31] using Becke−Lee−Yang−Parr (B3LYP)[32]/ωB97X-D[33] level of theory with 6-311++G(d,p) basis set. Frequencies were computed analytically for all the optimized species to characterize each stationary point minima. Gibbs free energy was employed in estimating relative energies.

Results and Discussion

Synthesis and Characterization

Aminoguanidine hydrochloride (1 mmol) was dissolved in water (2 mL) and to the stirred solution, NaOH pellets were added (5 mmol). The reaction mass was stirred to get clear solution, subsequently 2,6-dichlorobenzaldehyde (1 mmol) was added. The reaction mass was stirred at room temperature which resulted in the formation of precipitate of product in 1h. (Scheme 1).[19] The resultant precipitates were filtered and washed with water (2×2 mL) to remove the excess of

NaOH. The precipitates were dried under reduced pressure to afford guanabenz free base in 96 % yield. This synthetic procedure is different from the standard method in which protonated guanabenz is isolated.[34]

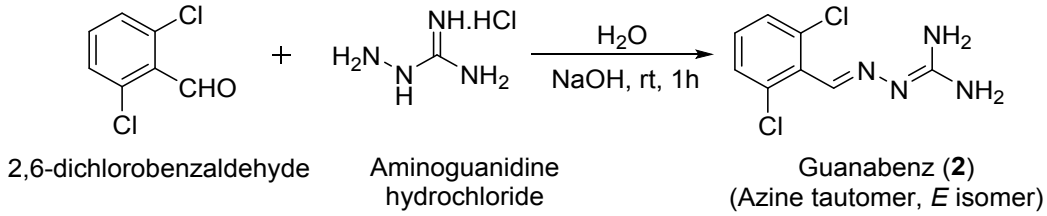

2,6-dichlorobenzaldehyde | Aminoguanidine hydrochloride | Guanabenz (**2**) (Azine tautomer, *E* isomer)

Scheme 1. Synthesis of guanabenz free base (**2**).

The characterization of the product by ^{1}H NMR spectroscopy in DMSO-d_6 confirms the formation of guanabenz in its preferred azine tautomeric state as it is evidenced from the presence of two broad singlets of two protons each at 5.81 ppm and 5.84 ppm which are the characteristic probe for the presence of azine tautomer.[19] Further, the confirmation for the presence of azine tautomer was provided by ^{13}C NMR spectroscopy where a signal at δ 161.98 ppm was observed which is attributed to the $C(NH_2)_2$ carbon, a characteristic probe of azine tautomer. From the ^{1}H NMR study, we observed the presence of only one isomer and it is assumed to be belong to the *E*-isomer of guanabenz.

When the compound was dissolved in pure methanol, suitable block shape crystals (Form I) started crystallizing out from pure methanol via slow evaporation at room temperature within 2 days and the yield kept on increasing subsequent days but there is no sign of Form II crystals in the same pot. The same observation occurs in pure water as solvent medium but the time duration is slightly longer as compared to pure methanol. Interestingly, a 5-10 % of water in methanol gave the first indication of existence of Form II, which appeared towards the end of the crystallization. However, the quality of the Form II crystals were very poor as well as brittle in nature. After several combination of mixture, it was found that the 3:1 mixture of methanol-water was the best

choice to improve the quality and yield of crystals of Form II along with Form I, however, the final yield ratio achieved is of 95:5 (Form I : Form II).

From the crystal data, it is clear that Form I has slightly higher density than Form II (Table 1) and the crystallization behavior is found to be very interesting. Either pure water or methanol yields Form I exclusively, while the mixture of solvents (MeOH: Water = 3:1) gives Form I and Form II with final yield ratio of 95:5. The above results are in well agreement with the observation by Diamant *et al.*, where Form I was obtained while crystallizing from pure water.[16] Again, it is found that Form I always crystalizes faster with good yields than Form II in methanol-water mixture with a time gap of more than two weeks. Keeping the crystallization till dryness of the solvent, results in lots of cracks on the surface of the Form I crystals. Both the high yield and fast crystalizing properties of Form I over Form II, might be the possible reasons because of which the existence of Form II was overlooked easily even though Form I has been known since 1985. Attempts to grow only Form II, was not successful in either of the pure solvent (methanol and water) and at the same time the screening of crystallization in other solvents like ethanol, acetonitrile, acetone, chloroform, ethyl acetate, and acetone gave no fruitful results mainly due to poor solubility. The block shaped Form I crystals are relatively harder while Form II crystals are rod shaped and fragile in nature. The quality of diffractions for Form II crystals are found to be very poor (diffracting to only low resolution) as compared to Form I, and as a result of, data quality could not be improved even after several attempts.

It is well known that seeding facilitates the crystallization process via heterogeneous or secondary nucleation. Attempts to obtain more crystals of Form II in the presence of few crystals of Form II to facilitate secondary nucleation, resulted in no further success and crystallizing properties remain same. It is again confirmed that Form I grows faster than the seed crystals and

crystallize out. As per the cross nucleation phenomena[35] several different solid state forms nucleate on each other and the state with a fastest growth rate will be eventually observed regardless of the rate of nucleation, in the present case this concept holds good for Form I.

Crystallographic and Structural Details

The two types of crystals can be separated mechanically from the same crystallization pot due to their distinct crystal morphology – Form I exclusively adopts block shape and Form II adopts rod shape. The optical photographs of the two forms show distinct crystal morphologies of the two isomers (Figure 3). The two forms show prominent dissimilarities in many aspects like crystal habits, molecular conformations and crystallization towards different solvent environment. In this contribution, we were thus presented with an opportunity for the comparison of the molecular assembly in the crystals of both the Forms, thermal studies and theoretical calculations.

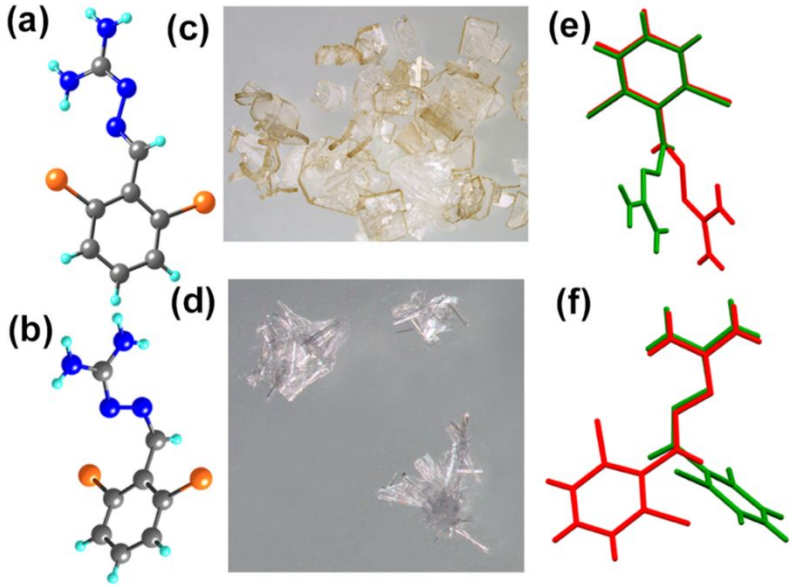

Figure 3. Ball and stick models of (a) Form I and (b) Form II; optical pictures of the crystals (c) Form I and (d) Form II; overlap diagrams of Form I and Form II at each ends showing level of mismatches (e-f, red: Form I, green: Form II).

Table 1 lists the cell parameters of Form I and Form II obtained in this study. A comparison of cell parameters of Form I has also been made with that of reported by Diamant *et al.* in 1985.[16] The cell parameters of the two forms are quite different with Z′ values (Form I, Z′ = 1; Form II, Z′ = 2; Table 1). The ORTEP plots of the two forms are provided in Figure 4.

Table 1. Comparison of cell parameters of the reported crystal structures of guanabenz Form I with Form II. Structural details of the reported structure (Form I) were not available in CCDC and hence a new data set collected to highlight the differences.

Compound	**Form I (*E*)**	**Form I (*E*)**	**Form II (*Z*)**
CCDC No.	not found	1866599	1866600
Reference	Reference-16	This work	This work
space group	$P2_1/c$	$P2_1/c$	*P*-1
T/K	unknown	293	293
a/Å	16.290	16.3082(4)	7.9018(3)
b/Å	8.309	8.2933(3)	10.8460(7)
c/Å	7.490	7.4489(3)	12.9559(8)
α/deg	90	90	72.515(4)
β/deg	98.34	98.201(3)	78.313(5)
γ/deg	90	90	83.119(4)
Z′/Z	1/4	1/4	2/2
V/Å^3	unknown	997.15(6)	1035.03(10)
D_{cal}/(gcm^{-3})	-do-	1.539	1.483
R_1[I>2σ(I)]	0.035	0.0426	0.0712
Reflns collected	unknown	7796	14259
Unique reflns	-do-	2112	4384
Observed reflns	-do-	1768	2410

$_{w}R_2$[all]	-do-	0.0988	0.2422
R_{int}	-do-	0.0324	0.0916
GOOF	-do-	1.054	1.114

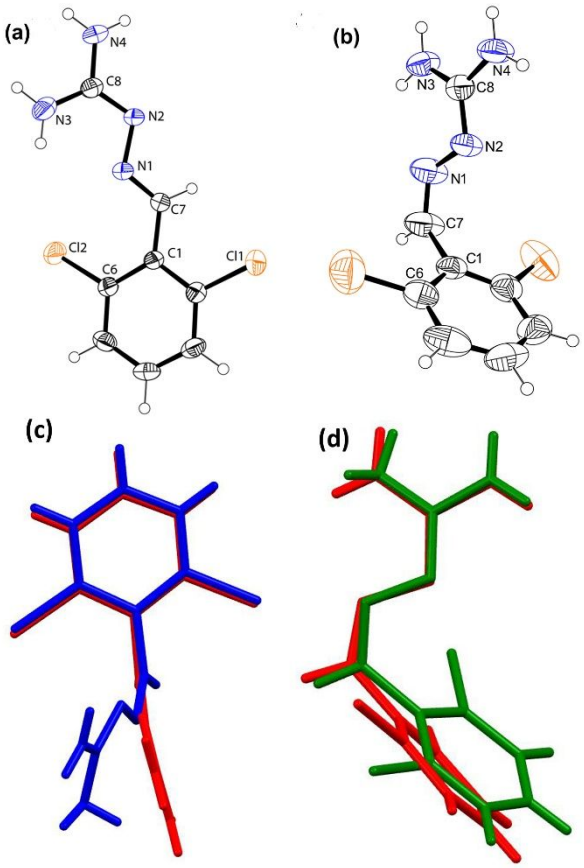

Figure 4. ORTEP diagram for (a) Form I and (b) Form II at 35% and 50 % probability ellipsoids respectively; (c) and (d) are the overlap diagram of the two independent molecules of Form II in different orientations.

There are clear differences between the crystal structures of Form I (zigzag chain of molecules) and Form II (planar and lamellar packing), apart from the fact that their unit cell parameters, space groups, and Z′ values are different. Form I is crystallized in the $P2_1/c$ symmetry and Form II is crystallized in P1 symmetry. Form I has only one molecule in asymmetric unit cell, in contrast, Form II has two molecules in the asymmetric unit cell. These two molecules of Form

II have difference in their geometry as it is evident by overlapping them in different orientation (Figure 4c, 4d). Although both Form I and Form II possess equal number of donor-acceptor sites (amino group-donor; imino group-acceptor), due to different flipping arrangement, in Form I, only one amino group of aminoguanidine group participates in H-bonding while in Form II both amino groups actively involved in H-bonding. As a result, in Form I there are two sets of H-bonds in total while three sets of H-bonds are present in Form II. It is well known that there is always a competition between directional interactions versus better packing in crystal engineering, which leads to different crystallization. There are reports which suggest that the solid state forms with looser packing and better H-bonding can lead to higher Z′ value and similar observation is found in Form II.[36,37]

From the structural study, it became clear that the differences in the two forms are due to *E*/*Z* isomerism across the C7-N1 bond. Further, the differences due to the rotation across C1-C7 single bond are also noticeable. The aromatic 2,6-dichlorophenyl ring and the methylene aminoguanidine moieties are planar individually and are arranged orthogonally to each other in Form II whereas they tend to be coplanar in Form I. The angle ϕ between the two planes is 82.34° and the corresponding angle for Form I is 40.32°. The overlap structures of the Form I and Form II reveal the level of mismatch of the forms after making a suitable alignment at any one end (aromatic group or guanidine moiety) creates the corresponding mismatch automatically in the other end (Figure 3e and 3f).

It is intriguing to note that only one isomer was noticed in the solution state (^{1}H NMR, Figure S11), whereas two forms observed in solid state (which are clearly distinguishable). To verify, both solid forms were dissolved in DMSO-d6 and subjected to ^{1}H NMR studies. The ^{1}H NMR spectra of Form I and Form II are provided in Figure 5. The ^{1}H NMR of the solid compound

obtained after synthesis (as synthesized, Figure S11) is identical as that of Form I confirming the presence of *E*-isomer in solution phase. The ^{1}H NMR spectrum of Form II exhibits distinct characteristic peaks. The chemical shift (δ) value of –CH=N proton in Form I and Form II appear at 8.20 ppm and 7.10 ppm respectively. A shifting of signal due –C**H**=N proton from 8.20 ppm (Form I) to 7.10 ppm (Form II) is due to the presence of nitrogen lone pair on the same side of proton nucleus in Form II causing its shielding, resulting into a shift of signal in upfield region. Thus, the two isomers can be easily distinguishable in solution state also.

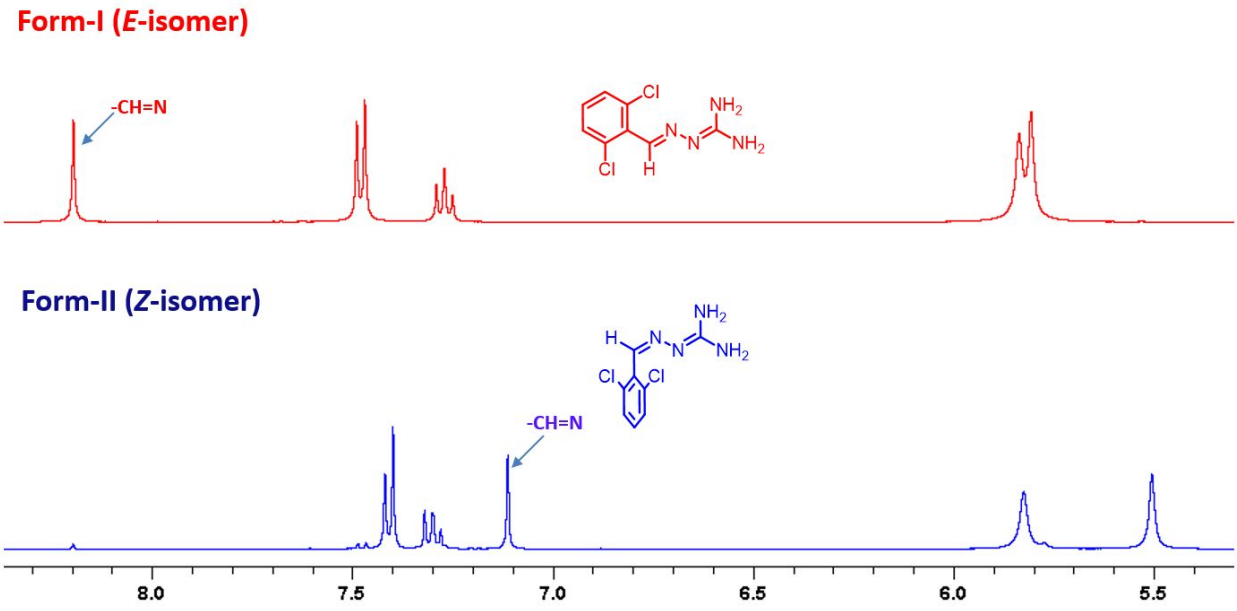

Figure 5. An overlay of ^{1}H NMR of Form I and Form II of guanabenz in DMSO-d_6.

Figures 6a and 6b show the interactions within the dimers of Form I and Form II respectively. In both cases the dimers are characterized by two intermolecular hydrogen bonds (~ 2.27 Å), leading to $R_2^2(8)$ supramolecular synthon. The differences between the two crystal structures are very clear in the dimers of Form I and Form II – In Form I, the phenyl groups are coplanar with the molecules and are away from the central synthon whereas in Form II, the phenyl groups flank the central synthon unit. In the crystal structures of Form I and Form II, repeated units

of tetramers exist (Figure 6c and 6d respectively) which are generally connected by two sets of H-bonds of N H···N type (Form I: 2.27, 2.74 Å; Form II: 2.27, 2.07 Å). Again for Form I, each dimer unit is connected via π···π interactions (3.61Å, centroid-centroid) (Figure 6e) and extends the chain along *bc*-plane. Similarly, π–π stacking interactions between molecules are clear in Form II also, which become apparent only when the molecular assembly is considered beyond tetrameric state (Figure 6d vs. 6f)

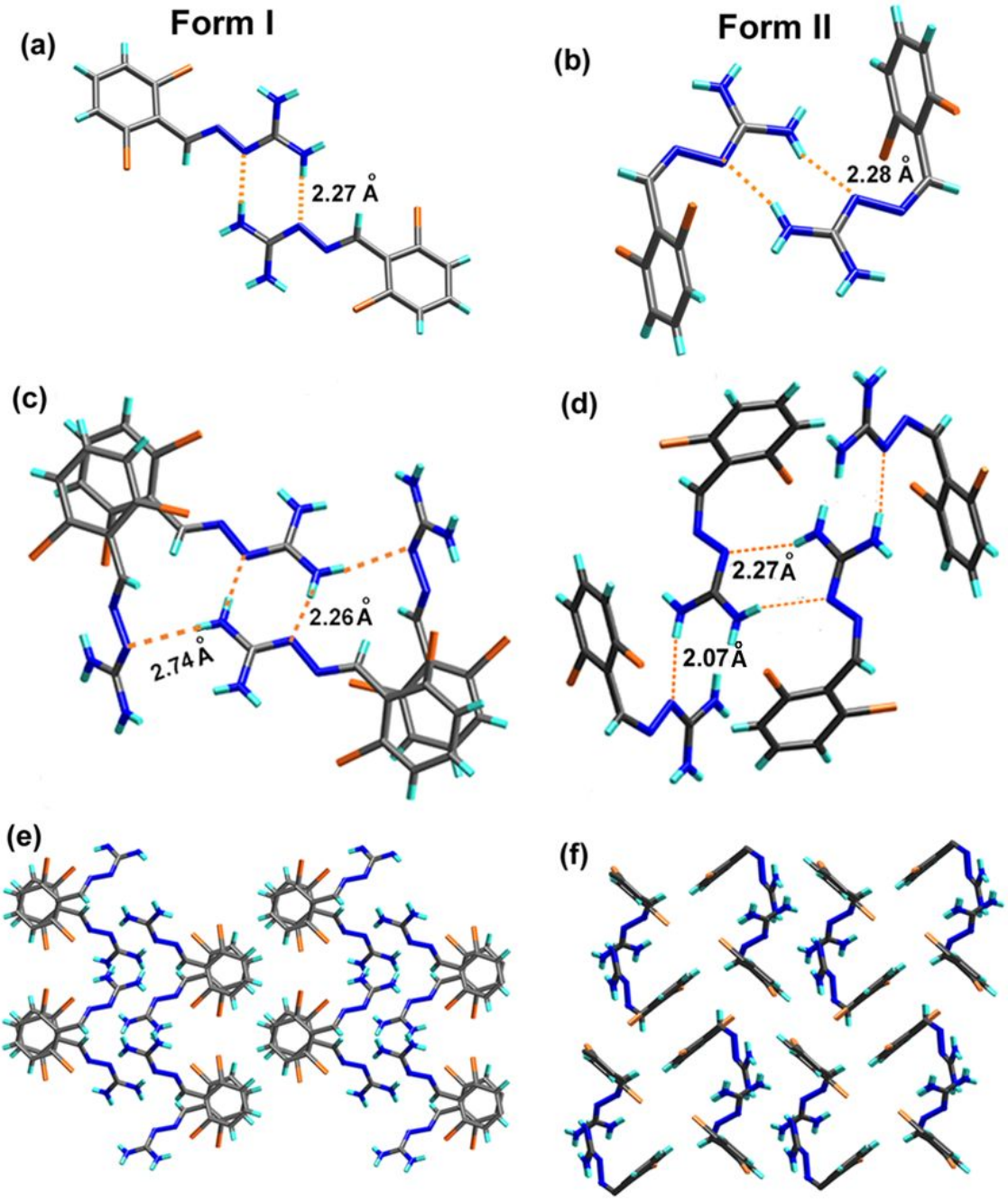

Figure 6. Hydrogen bonding and molecular packing in the crystal structures of guanabenz Form I (left panel) and Form II (right panel).

The 2D fingerprint plots as a Hirshfeld surface[38-40] for the two forms display various interactions as the main structure governing the N4 H···N2 hydrogen bond is the same in both the structures, confirmed by a pair of sharp spikes in the plots (Figure 7). The relative contributions

of each interaction to the Hirshfeld surface are shown in Figure-S7. Both the forms have almost similar N···H, Cl···H and H···H interactions, however Form II has less C···C contacts compared to Form I (Figure 7). The presence of π-π stacking interaction is more prominent in case of Form I which is evidenced by comparing the crystal structures and the Hirshfeld finger print plots.

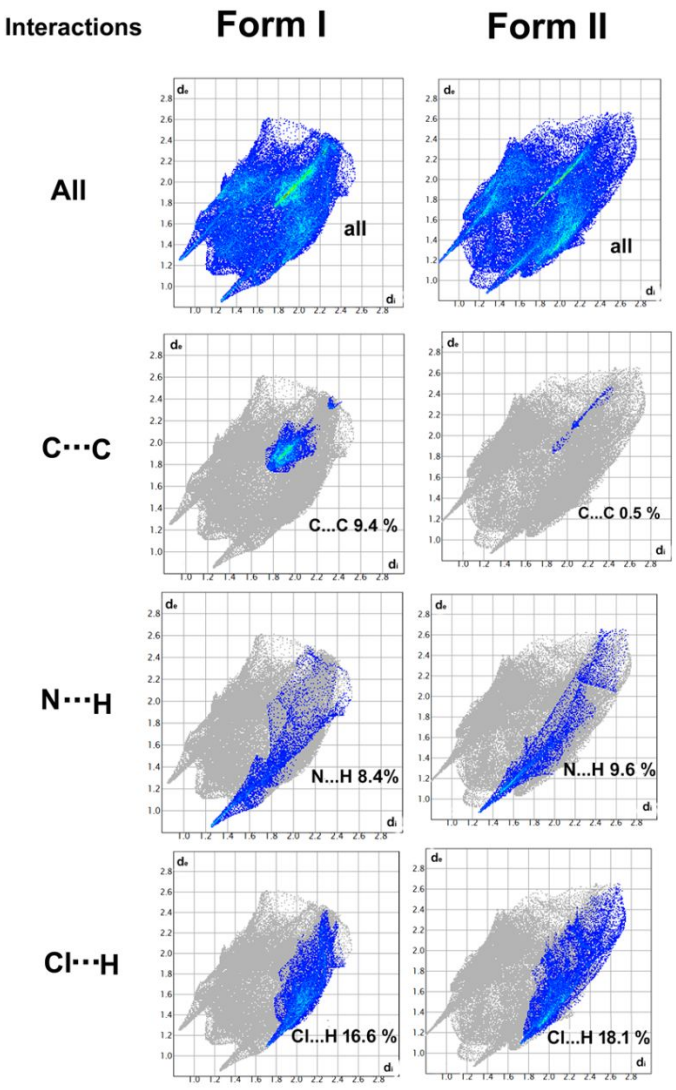

Figure 7. 2D fingerprint Hirshfeld surfaces plots of Form I and Form II showing the various interactions and their percentage.

FTIR and PXRD Analyses

The IR spectra of two forms are shown in Figures S4-S6. There are several strong and distinct transmittance bands for Form I and II and can be easily comparable. As shown in Figure S4, for Form I the peaks are in the region 2917 cm^{-1} (N=C-**H**), 1594 cm^{-1} (C=N) and 840 cm^{-1}(C-Cl), 660 cm^{-1} (N=C-**H**, Bending). Form II does not show any peak near 2917 cm^{-1}, whereas the other two signals are partly shifted at 1592 cm^{-1}, 862 cm^{-1} and 671 cm^{-1}. One significant difference is due to the iminic C-H stretch. In Form I, the C-H bond of the imine group shows distinct signals (2917 cm^{-1}) as it is not involved in any kind of interactions in the crystal structure. On the other hand, in Form II, the iminic C-H bond is involved in a C-H···Cl type interaction, thus the vibrational frequency is not sufficiently free to exhibit peak in IR spectrum (Figure S5). This observation is in good agreement with the Hirshfield analysis also (Figure S7).

A comparison of experimental PXRD pattern of Form I, Form II and mixture reveals the differences in the crystal arrangement and phase of the two Forms (Figure 8). After physically separating the two forms and/or exclusive isolation of Form I, the experimental and simulated PXRD patterns were compared (Figure S1 and S2). The experimental patterns match well with the simulated ones, confirming the phase purity of the physically separated forms. After successfully isolating the two forms in the same pot, the mixture was subjected to PXRD analysis (Figure S3). The PXRD pattern shows distinctive peaks coming from each form as well as percentage of each isomer. At least in three different instances of isolation of mixture, we observed that the percentage of Form I isomer varies between 80-95 % and can be clearly observed both under optical microscopy (Figure S10) as well as in PXRD analysis.

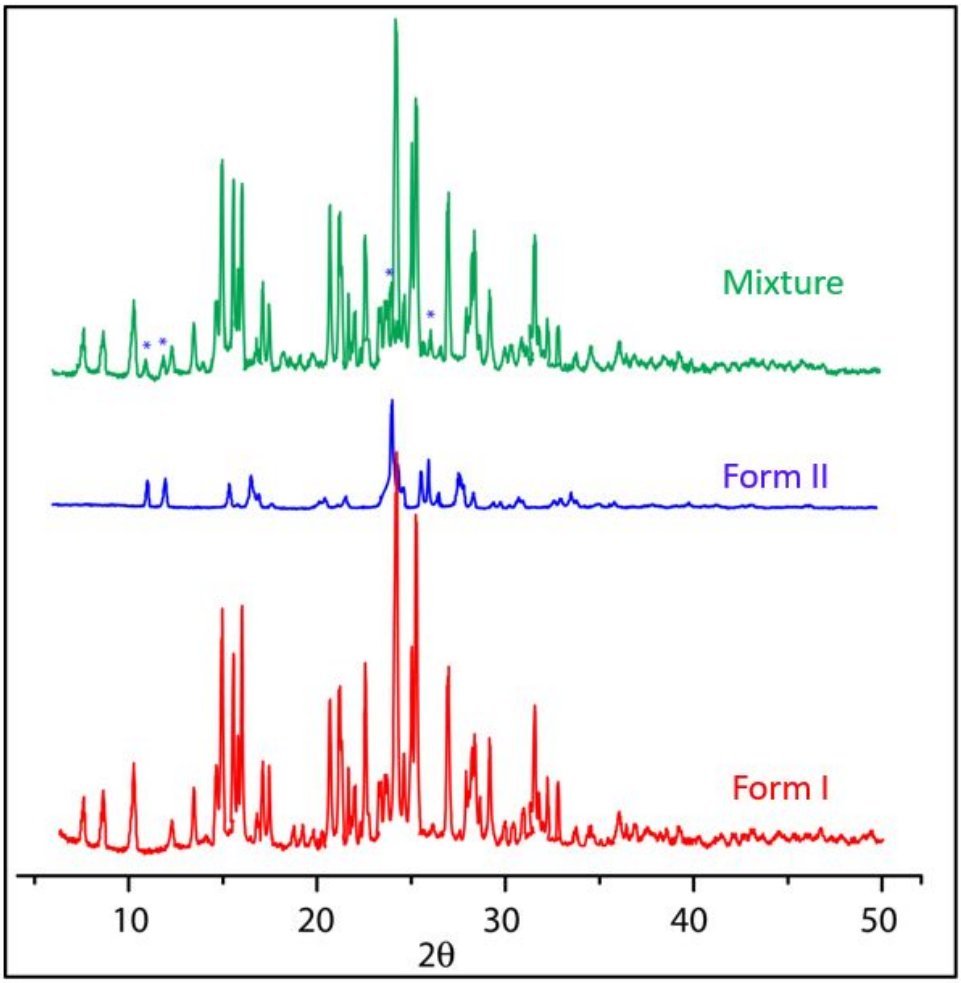

Figure 8. Experimental PXRD pattern of Form I (red), Form II (blue) and mixture (green).

Thermal Analysis of Form I and II

The thermograms of Form I and II give almost identical thermal signatures (Figure 9). There are horizontal plateau without any weight loss which confirms the stability of the two forms till 250 ºC. However, after 250 ºC both the forms start decomposing, this process is faster for Form II in comparison to Form I. At around 550 ºC, both forms of the guanabenz decomposed completely. From the thermogram plot, it is clear that the both the isomers of guanabenz melting starts nearly at ~230 ºC and it is matching exactly with the value of 227 ºC for Form I isomer reported by Diamant *et al*.[16] A good correlation can be observed from the crystal structure of both the Forms.

In Form I, the molecules are held tightly by strong H-bonds (2.27 Å) as compared to Form II (2.28, 2.0 Å) with an additional π···π stacking interactions (Figure 6c) as a result more energy may require to make the molecules free.

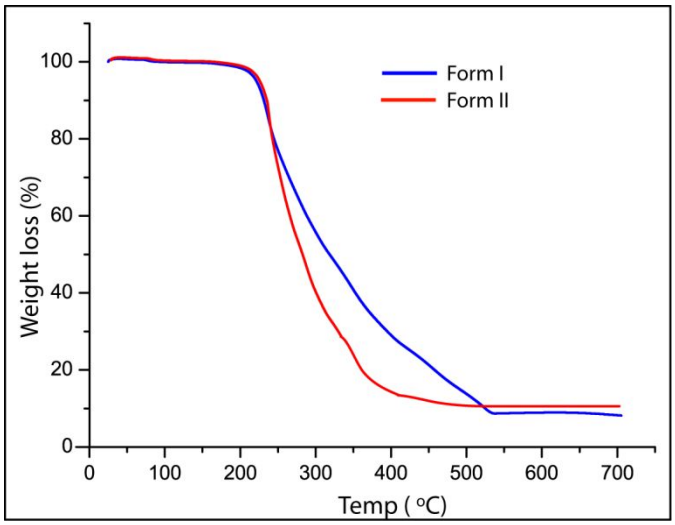

Figure 9. Thermogravimetric analysis (TGA) plots of Form I (blue) and Form II (red).

DSC Analysis

The DSC profile for Form I shows weak endotherm around 61.7 °C followed by a weak exotherm at 215 °C and finally the compound decomposed at 318 °C (Figure S8). Apart from that, Form I also shows a few unresolved multiple weak peaks between 110-160 °C which may be due to the association of martensitic phase transition.[41] On the other hand, the DSC profile of Form II is rather smooth till 215 °C and the compound shows a sharp endotherm (217 °C) related to melting of the compound followed by an immediate exotherm (225 °C) with just a gap of 8 °C correspond to the oxidative degradation (Figure S9). Comparing the TGA and DSC profiles of Form II, it is clear that the first endotherm occurs at 217 C which is very much consistent with the decomposition temperature of ~220℃ obtained from TGA data. Although melting of both Form I and Form II starts nearly at the same temperature, the TGA profile of both the forms are quite distinguishable. The Form II shows a sharp fall in weight loss (200-350℃) as compared to Form I

which shows a gradual rate of decomposition at temperature 200-500 ℃. Comparing the whole range of decomposition, we assume that Form I is little more thermodynamically stable than Form II.

Quantum Chemical Analysis

To understand the driving factors for the observed isomers in guanabenz, quantum chemical calculations were performed. Initially, the calculations were performed on the monomers of guanabenz (*E*- and *Z*- isomers). The results from B3LYP/6-311+G(d,p) analysis suggested that the *E*-isomer (Form I) is more stable than the *Z*-isomer (Form II) by 2.13 kcal/mol suggesting that the *E*-isomer is thermodynamically more stable than *Z*-isomer. GIAO (Gauge-Independent Atomic Orbital) method was employed to estimate the chemical shift values. The chemical shift value for the iminic proton of *E*-isomer and *Z*-isomer is 8.81 and 7.57 ppm respectively which is consistent with the experimentally obtained chemical shift values. The N1-inversion barrier (also the –C7=N1 rotational barrier) for the *E*/*Z* isomerization is ~37 kcal/mol. The N1-inversion barrier after protonation is ~39 kcal/mol, suggesting that the inversion process is thermodynamically prohibited between the *E* and *Z* isomers in guanabenz. Since guanabenz is highly basic, it prefers to exist in protonated state. Quantum chemical analysis showed that the proton affinity (PA) values for the *E* and *Z* isomers are 237 and 238 kcal/mol respectively showing the highly basic character for both the isomers. The intrinsic energy difference (2.13 kcal/mol) may be the driving force for observing the *Z*-isomer as the minor isomer in the mixture. Considering that only one isomer is found in the reaction product and also considering that the *E*/*Z* conversion is an energetically prohibited process, it is intriguing that Form II is found in solid state. To explore this, the dimeric states of the *E*- and *Z*-isomers of guanabenz are also studied using quantum chemical methods. Since, the DFT-B3LYP functional cannot adequately account for the dispersion interactions (non-bonding)

the dispersion corrected DFT functional i.e. ωB97X-D[33] was used to calculate the energy differences between both the isomers in their dimeric state.

The 3D structures of dimers according to ωB97X-D based geometry optimization are given in Figures 10a and 10b. According to the crystal structure data (Figure 6a and 6b), the intermolecular hydrogen bonds in *E* and *Z* dimers are of the order of approximately 2.28 Å. According to the gas phase calculations, these intermolecular hydrogen bond lengths are much shorter (1.93 Å in the *E*-isomer and 1.92 Å in the *Z*-isomers). In the crystal structure, an η^2 type of cation-π interaction has been noticed for *Z*-dimer. In the optimized *Z*-dimer, an η^6 type of cation-π interaction (~3.2 Å) has been noticed. The stabilization energies due to the dimer formation in the *E*-isomer is 2.21 kcal/mol. The stabilization energy due to the dimer formation in *Z*-isomer is 4.89 kcal/mol. This greater stabilization in *Z*-isomer (2.68 kcal/mol) can be attributed to the strong cation-π interaction. This is also reflected in the greater stability of the *Z*-dimer (by 1.45 kcal/mol).

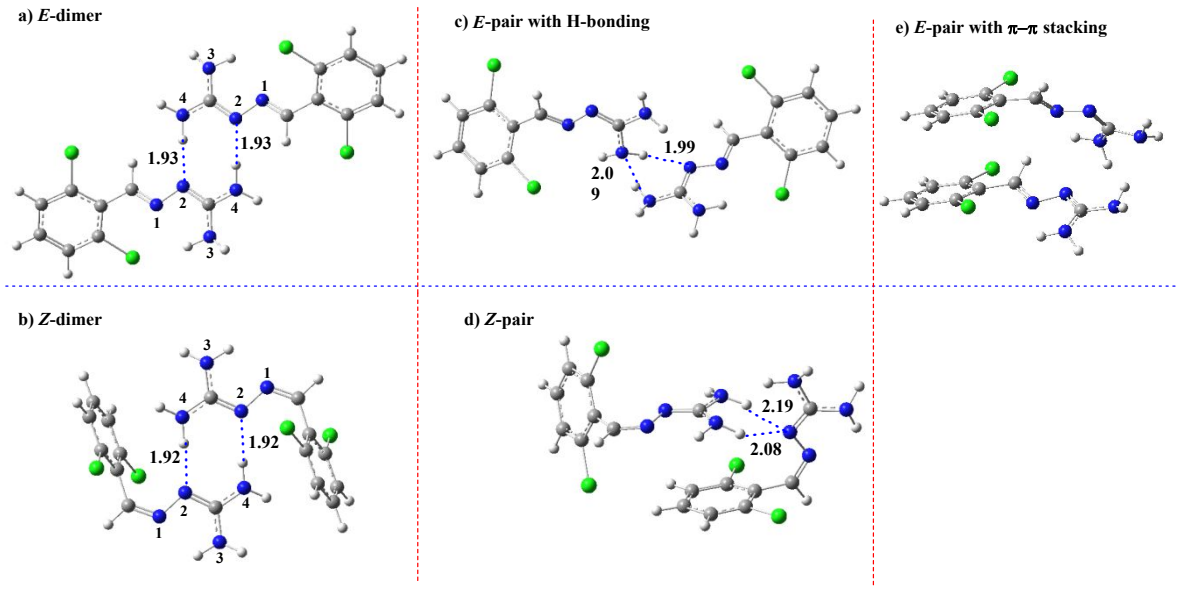

Figure 10. The optimized 3D structures of *E*, *Z*-dimers (a,b) and *E*, *Z*-pairs (c-e). The dotted lines represents the hydrogen bond interactions and the distances are in Å.

The tetrameric states of Form I and Form II (Figure 6c and 6d) clearly indicate the presence of additional set of intermolecular hydrogen bond interactions between the pairs of monomers. To estimate the strength of these additional interactions the 3D geometries of these pairs are extracted from the crystal structure and further subjected to geometry optimization. The optimized 3D structures of these pairs (*E*-pair and *Z*-pair) are given in Figures 10c and 10d respectively. An additional pair of *E*-isomer was also considered i.e. *E*-pair with π- π stacking interaction due to arene moieties (Figure 10e). In the *E*-pair (Figure 10c), two intermolecular hydrogen bonds of lengths 1.99 Å and 2.09 Å are found according to the quantum chemical study. However, in the *Z*-pair (Figure 10d), bifurcated hydrogen bonds of the order of 2.08 Å and 2.19 Å have been noticed along with cation-π interaction. The stabilization energy due to the *E*- pair formation with H-bonding is 1.49 kcal/mol. In case of *E*-pair with π- π stacking interaction, the energy gain due to pair formation is only 0.30 kcal/mol suggesting that π-π stacking interaction is playing a minor role in the stabilization of *E* pair. The stabilization energy due to pair formation in *Z*-isomer is 5.79 kcal/mol, this stabilization energy is relatively larger compared to *E*-pair with H-bonding and π- π stacking interaction, this result further suggests that the cation-π interaction present in *Z*-dimer and *Z*-pair is playing crucial role in their stabilizing them in the solid state. Hence, the overall extra stabilization due to dimer (2.68 kcal/mol) and pair formation (4.00 kcal/mol) in the *Z*-isomer is of the order of the ~7 kcal/mol for each molecule of guanabenz. Though, the *Z*-isomer is less stable than *E*-isomer in monomeric state, it experiences extra stability (hydrogen bonding and hydrophobic interactions) in the solid state due to intermolecular interactions. In addition, added advantages, presumably due to hydrophobic contacts, crystal packing forces might be contributing to the observation of Form II of guanabenz.

Isomerism vs. Polymorphism

Different crystalline states of a chemical substance are known as polymorphs. Polymorphism observed due to conformational differences in the structure in solid state leads to conformational polymorphism. Tautomeric difference observed in solid state leads to tautomeric polymorphism. Though there is "a need for clear definition of polymorphism there is an implied correspondence between different molecular arrangements and different crystal forms".[42,43] Especially, when the information from solid state studies leads to the identification of two different arrangements, the use of the term polymorphism is quite justified.

In the current work, the two different molecular arrangements of the drug guanabenz were identified "from the solid state information to the structure information" rather than "from the structural information to the solid state information" i.e. From I and Form II of guanabenz free base were first identified which further lead to the identification of *E*/*Z* isomerism in guanabenz. Thus, Form I and Form II may be considered as two polymorphs of same molecule and the origin of the observed polymorphism has been attributed to the differences in the geometrical arrangements of atoms. In such context it may be worth considering the two polymorphs as configurational polymorphs,[44,45] on the same lines as that of "conformational polymorphs" and that of "tautomeric polymorphism".[46] The observation of polymorphism due to geometrical isomers was earlier reported by a few scientific groups – for ex. Configurational isomerism and polymorphism in chalcones reported by Xu and coworkers.[47]

Conclusions

In summary, it was demonstrated that guanabenz can exist in two forms (Form I and Form II), the two forms differ in terms of their geometry across –C=N. The *E* isomer is thermodynamically more stable and lead to the major polymorph i.e. Form I. The *Z* isomer, which

is 2.13 kcal/mol less stable leads to the formation of the minor polymorph (Form II). In both the forms, guanabenz exists exclusively in an azine tautomeric state, in contrast to the general perception i.e. it is a hydrazone derivative. In solution state (NMR analysis in DMSO-d_6), only one form was noticed with *E* geometry, however, after crystallization the ^{1}H NMR of both isomers could be recorded. Both the isomers can be separated by mechanical means due to their distinct crystal morphology – (i) Form I exclusively adopts a block shaped arrangement, (ii) Form II adopts a rod shaped arrangement. Both the forms were characterized by single crystal XRD. The single crystal and powder XRD studies clearly show the differences between the two forms. The quantum chemical analysis was carried out on the dimers of the Form I and Form II to rationalize their existence in the solid state, to explore the energy as well as electronic factors associated with the two forms.

Experimental

(*E*)-4-(2,6-dichlorophenyl)-1,1-diamino-2,3-diazabuta-1,3-diene (2)

White solid (315 mg, 96%). mp 220-222 °C; IR (KBr, cm^{-1}): 3358, 1663, 1538, 1148; ^{1}H NMR (400 MHz, DMSO-*d6*) δ 8.20 (s, 1H), 7.49-7.55 (d, J = 8.2 Hz, 2H), 7.25 (t, J = 7.2 Hz, 1H); 5.81 (br s, 2H), 5.84 (br s, 2H); ^{13}C NMR (100 MHz, DMSO-*d6*) δ 161.98, 137.86, 133.72, 132.22, 129.68, 129.25; HRMS (ESI-TOF) *m/z*: $[M+H]^+$ Calcd for $C_8H_9Cl_2N_4$ 231.0198; Found 231.0195.

ASSOCIATED CONTENT

Supporting information

Experimental details, X-ray crystallography, crystal structure analysis, thermal analysis, and CIF files. The coordinates of the quantum chemically optimized geometries of monomers and dimers of the Form I and Form II of guanabenz are also included along with their absolute energies. CCDC 1557940 and 1870736, contain the supplementary crystallographic data for this paper. These data can be obtained free of charge via www.ccdc.cam.ac.uk.

AUTHOR INFORMATION

Corresponding Author

*E-mail: pvbharatam@niper.ac.in; subash.chem@gmail.com

Notes

The authors declare no competing financial interest.

ACKNOWLEDGEMENTS

Authors acknowledge DST-INSPIRE, New Delhi and CSIR, New Delhi for financial support. SCS thanks DST-FIST for single crystal facility at Panjab University.

REFERENCES

(1) Baum, T.; Eckfeld, D. K.; Metz, N.; Dinish, J. L.; Rowles, G.; van Pelt, R.; Shropshire, A. T.; Fernandez, S. P.; Gluckman, M. I.; Bruce, W. F. 2, 6-Dichlorobenzylidene amino guanidine acetate (Wy-8678). A new hypotensive agent. *Experientia* **1969**, *25*, 1066-1067.

(2) Baum, T.; Shropshire, A. T. Studies on the centrally mediated hypotensive activity of guanabenz. *Eur. J. Pharmacol.* **1976**, *37*, 31-44.

(3) Nash, D. T. Clinical trial with guanabenz, a new antihypertensive agent. *J. Clin. Pharmacol. New Drugs,* **1973**, *13*, 416-421.

(4) Wishart, D. S.; Feunang, Y. D.; Guo, A. C.; Lo, E. J.; Marcu, A.; Grant, J. R.; Sajed, T.; Johnson, D.; Li, C.; Sayeeda, Z. DrugBank 5.0: a major update to the DrugBank database for 2018. *Nucleic Acids Res.* **2017**, *46*, D1074-D1082.

(5) Norez, C.; Vandebrouck, C.; Antigny, F.; Dannhoffer, L.; Blondel, M.; Becq, F. Guanabenz, an α2-selective adrenergic agonist, activates Ca2+-dependent chloride currents in cystic fibrosis human airway epithelial cells. *Eur. J. Pharmacol.* **2008**, *592*, 33-40.

(6) Neuber, C.; Uebeler, J.; Schulze, T.; Sotoud, H.; El-Armouche, A.; Eschenhagen, T. Guanabenz interferes with ER stress and exerts protective effects in cardiac myocytes. *PLoS One* **2014**, *9*, e98893.

(7) Da, C. L. E.; da Rosa Santos, O. Silvestre Labs Química E Farmaceutica Ltda., 2012. Guanabenz-containing compound for the treatment of primary cutaneous amyloidosis.

(8) Gug, F.; Oumata, N.; Tribouillard-Tanvier, D.; Voisset, C.; Desban, N.; Bach, S.; Blondel, M.; Galons, H. Synthesis of conjugates of 6-Aminophenanthridine and guanabenz, two

structurally unrelated prion inhibitors, for the determination of their cellular targets by affinity chromatography. *Bioconjugate Chem.* **2010**, *21*, 279-288.

(9) Tribouillard-Tanvier, D.; Béringue, V.; Desban, N.; Gug, F.; Bach, S.; Voisset, C.; Galons, H.; Laude, H.; Vilette, D.; Blondel, M. Antihypertensive drug guanabenz is active in vivo against both yeast and mammalian prions. *PloS one* **2008**, *3*, e1981.

(10) Nguyen, P. H.; Hammoud, H.; Halliez, S.; Pang, Y.; Evrard, J.; Schmitt, M.; Oumata, N.; Bourguignon, J.-J.; Sanyal, S.; Beringue, V. Structure–activity relationship study around guanabenz identifies two derivatives retaining antiprion activity but having lost α2-adrenergic receptor agonistic activity. *ACS Chem. Neurosci.* **2014**, *5*, 1075-1082.

(11) Chang, J.; Blazek, E.; Skowronek, M.; Marinari, L.; Carlson, R. P. The antiinflammatory action of guanabenz is mediated through 5-lipoxygenase and cyclooxygenase inhibition. *Eur. J. Pharmacol.* **1987**, *142*, 197-205.

(12) Takigawa, S.; Chen, A.; Nishimura, A.; Liu, S.; Li, B.-Y.; Sudo, A.; Yokota, H.; Hamamura, K. Guanabenz downregulates inflammatory responses via eIF2α dependent and independent signaling. *Int. J. Mol. Sci.* **2016**, *17*, 674.

(13) Tsuijkawa, T.; Mizuta, E.; Hayashi, M. Studies on heterocyclic compounds. IV. Geometrical isomers of 2-(2, 6-dichlorobenzylidenehydrazino)-1, 4, 5, 6-tetrahydropyrimidine hydrochloride and its related hydrazones. *Yakugaku Zasshi* **1976**, *96*, 125-131.

(14) Holzer, W.; Györgydeák, Z. On the structure of guanylhydrazones derived from aromatic aldehydes. *Monatsh. Chem.* **1992**, *123*, 1163-1173.

(15) Tanaka, R.; Hirayama, N. Crystal Structure of Guanabenz Acetate. *Anal. Sci.: X-Ray Struct. Anal. Online* **2008**, *24*, x5-x6.

(16) Diamant, S.; Agranat, I.; Goldblum, A.; Cohen, S.; Atlas, D. β-adrenergic activity and conformation of the antihypertensive specific α2-agonist drug, guanabenz. *Biochem. Pharmacol.* **1985**, *34*, 491-498.

(17) Mutikainen, I.; Elo, H.; Tilus, P. Crystal and Molecular Structures of the Free Base and the Monohydrochloride Salt of the Antileukemic Agent Glyoxal bis (Amidinohydrazone)[Glyoxal bis (Guanylhydrazone)']. *Z. Naturforsch. B* **1993**, *48*, 1821.

(18) Ramakrishnan, A.; Chourasiya, S. S.; Bharatam, P. V. Azine or hydrazone? The dilemma in amidinohydrazones. *RSC Adv.* **2015**, *5*, 55938-55947.

(19) Chourasiya, S. S.; Kathuria, D.; Nikam, S. S.; Ramakrishnan, A.; Khullar, S.; Mandal, S. K.; Chakraborti, A. K.; Bharatam, P. V. Azine-Hydrazone Tautomerism of Guanylhydrazones: Evidence for the Preference Toward the Azine Tautomer. *J. Org. Chem.* **2016**, *81*, 7574-7583.

(20) Kathuria, D.; Chourasiya, S. S.; Mandal, S. K.; Chakraborti, A. K.; Beifuss, U.; Bharatam, P. V. Ring-chain isomerism in conjugated guanylhydrazones: Experimental and theoretical study. *Tetrahedron*, **2018**, *74*, 2857-2864.

(21) Chourasiya, S. S.; Kathuria, D.; Singh, S.; Sonawane, V. C.; Chakraborti, A. K.; Bharatam, P. V. Design, synthesis and biological evaluation of novel unsymmetrical azines as quorum sensing inhibitors. *RSC Adv*., **2015**, 5, 80027-80038.

(22) Glaser, R.; Chen, G. S.; Barnes, C. L. Conjugation in azines. Stereochemical analysis of benzoylformate azines in the solid state, in solution, and in the gas phase. *J. Org. Chem.* **1993**, *58*, 7446-7455.

(23) Lewis, M.; Glaser, R. The azine bridge as a conjugation stopper: an NMR spectroscopic study of electron delocalization in acetophenone azines. *J. Org. Chem.* **2002**, *67*, 1441-1447.

(24) McLoughlin, C.; Clyburne, J. A.; Weinberg, N. Azines: conjugation stoppers or conjugation switches. *J. Mater. Chem*., **2007**, *17*, 4304-4308.

(25) Chen, G. S.; Anthamatten, M.; Barnes, C. L.; Glaser, R. Polymorphism and C=N-N=C Conformational Isomers of Azines: X-ray Crystal and Ab Initio Structures of Two Rotational Isomers of Methyl (para-Tolyl) Ketone Azine. *Angew. Chem., Int. Ed. Engl.*, **1994**, *33*, 1081-1084.

(26) Dolomanov, O. V.; Bourhis, L. J.; Gildea, R. J.; Howard, J. A.; Puschmann, H. OLEX2: a complete structure solution, refinement and analysis program. *J. Appl. Crystallogr.* **2009**, *42*, 339-341.

(27) Burla, M. C.; Caliandro, R.; Camalli, M.; Carrozzini, B.; Cascarano, G. L.; De Caro, L.; Giacovazzo, C.; Polidori, G.; Siliqi, D.; Spagna, R. IL MILIONE: a suite of computer programs for crystal structure solution of proteins. *J. Appl. Crystallogr.* **2007**, *40*, 609-613.

(28) Sheldrick, G. M. SHELXT–Integrated space-group and crystal-structure determination. *Acta Crystallogr., Sect. C: Struct. Chem.* **2015**, *71*, 3-8.

(29) Turner, M.; McKinnon, J.; Wolff, S.; Grimwood, D.; Spackman, P.; Jayatilaka, D.; Spackman, M. CrystalExplorer 3.0; University of Western Australia: Perth, Australia, 2012.

(30) Frisch, M. J.; Trucks, G. W.; Schlegel, H. B.; Scuseria, G. E.; Robb, M. A.; Cheeseman, J. R.; Scalmani, G.; Barone, V.; Mennucci, B.; Petersson, G. A.; Nakatsuji, H.; Caricato, M.; Li, X.; Hratchian, H. P.; Izmaylov, A. F.; Bloino, J.; Zheng, G.; Sonnenberg, J. L.; Hada, M.; Ehara, M.; Toyota, K.; Fukuda, R.; Hasegawa, J.; Ishida, M.; Nakajima, T.; Honda, Y.; Kitao, O.; Nakai, H.; Vreven, T.; Montgomery, J. A., Jr.; Peralta, J. E.; Ogliaro, F.; Bearpark, M.; Heyd, J. J.; Brothers, E.; Kudin, K. N.; Staroverov, V. N.; Kobayashi, R.; Normand, J.; Raghavachari, K.; Rendell, A.; Burant, J. C.; Iyengar, S. S.; Tomasi, J.; Cossi, M.; Rega, N.; Millam, J. M.; Klene, M.; Knox, J. E.; Cross, J. B.; Bakken, V.; Adamo, C.; Jaramillo, J.; Gomperts, R.; Stratmann, R. E.; Yazyev, O.; Austin, A. J.; Cammi, R.; Pomelli, C.; Ochterski, J. W.; Martin, R. L.; Morokuma, K.; Zakrzewski, V. G.; Voth, G. A.; Salvador, P.; Dannenberg, J. J.; Dapprich, S.; Daniels, A. D.; Farkas, Ö.; Foresman, J. B.; Ortiz, J. V.; Cioslowski, J.; Fox, D. J. *Gaussian 09, Revision D.01*; Gaussian, Inc., Wallingford CT, 2009.

(31) Parr, R. G.; Yang, W. *Density-Functional Theory of Atoms and Molecules* New York: Oxford University Press, 1989.

(32) Lee, C.; Yang, W.; Parr, R. G. Development of the Colle-Salvetti correlation-energy formula into a functional of the electron density. *Phys. Rev.* **1988**, *37*, 785-789.

(33) Chai, J. D.; Head-Gordon, M. Long-range corrected hybrid density functionals with damped atom–atom dispersion corrections. *Phys. Chem. Chem. Phys.*, **2008**, *10*, 6615-6620.

(34) Shearer, C. M. Guanabenz acetate. InAnalytical Profiles of Drug Substances. *Anal. Profiles Drug Subst.*, **1986**, *15*, 319-336.

(35) Tao, J.; Jones, K. J.; Yu, L. Cross-nucleation between D-mannitol polymorphs in seeded crystallization. *Cryst. Growth Des.* **2007**, *7*, 2410-2414.

(36) Chandran, S. K.; Nangia, A. Modulated crystal structure (Z′= 2) of α-d-glucofuranose-1, 2: 3, 5-bis (p-tolyl) boronate. *CrystEngComm*, **2006**, *8*, 581-585.

(37) Desiraju, G. R. On the presence of multiple molecules in the crystal asymmetric unit (Z′> 1). *CrystEngComm*, **2007**, 9, 91-92.

(38) McKinnon, J. J.; Jayatilaka, D.; Spackman, M. A. Towards quantitative analysis of intermolecular interactions with Hirshfeld surfaces. *Chem. Commun.* **2007**, 3814-3816.

(39) Spackman, M. A.; Jayatilaka, D. Hirshfeld surface analysis. *CrystEngComm* **2009**, *11*, 19-32.

(40) Bernstein, J. Polymorphism− a perspective. *Cryst. Growth Des.* **2011**, *11*, 632-650.

(41) Wu, H.; West, A. Thermally-induced homogeneous racemization, polymorphism, and crystallization of pyroglutamic acid. *Cryst. Growth Des*. **2011**, *11*, 3366-3374.

(42) Rogers, R. D. Introduction: Polymorphism in crystals. *Cryst. Growth Des*. **2003**, *6*, 867-867.

(43) Desiraju, G. R. Polymorphism: the same and not quite the same. *Cryst. Growth Des*. **2008**, *8*, 3-5.

(44) Cruz-Cabeza, A. J.; Bernstein J. Conformational polymorphism. *Chem. Rev*., **2013**, *114*, 2170-2191.

(45) Nangia, A. Conformational polymorphism in organic crystals. *Acc. Chem. Res.*, **2008**, *41*, 595-604.

(46) P. M. Bhatt and Desiraju G. R. Tautomeric polymorphism in omeprazole. *Chem. Comm.*, **2007**, *20*, 2057-2059.

(47) Zhang R.; Wang M.; Sun H.; Khan A.; Usman R.; Wang S., Gu X.; Wanga J.; Xu C. Effect of configurational isomerism and polymorphism on chalcone fluorescent properties. *New J. Chem.*, **2016**, *40*, 6441-6450.

For Table of Contents Use Only

Geometrical Isomerism in Guanabenz Free Base: Synthesis, Characterization, Crystal Structure and Theoretical Studies

Deepika Kathuria, Sumit S. Chourasiya, Aabid Abdullah Wani, Manjeet Singh, Subash C. Sahoo and Prasad V. Bharatam

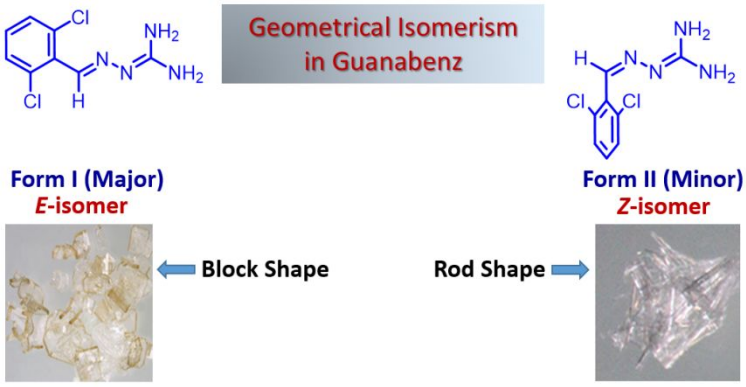

Brief Synopsis

The *E*/*Z* isomerism in guanabenz free base is responsible for the identification of two solid forms i.e. Form I (*E*-isomer) and Form II (*Z*-isomer). These two forms may be consider as geometrical polymorphs. Quantum chemical analysis and 2D fingerprint plots as Hirshfeld surfaces of these two forms highlight the differences in intermolecular hydrogen bonding, energy differences and π- stacking interactions.

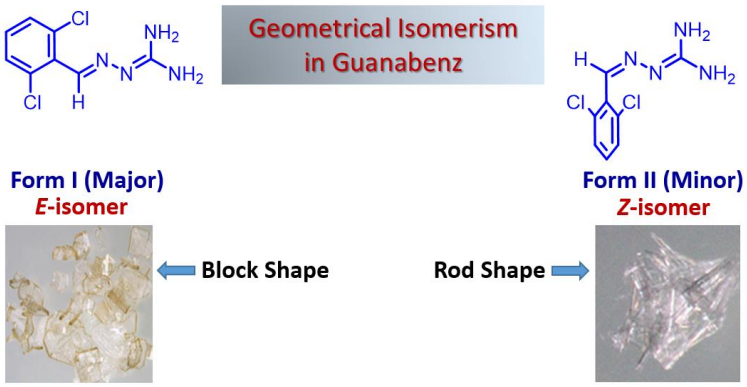
Geometrical Isomerism in Guanabenz
Form I (Major)
E-isomer
Block Shape
Rod Shape
Form II (Minor)
Z-isomer